A note on the representation of rate-of-rise of the thermal stratification interface in reactor plenum

(Research Report)

September, 1999

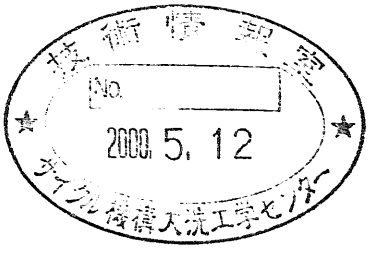

Japan Nuclear Cycle Development Institute

O-arai Engineering Center

Ⓚ

JNC TN9400 2000−015
September, 1999

A note on the representation of rate-of-rise of the thermal stratification interface in reactor plenum

A. Tokuhiro[1] and N. Kimura[2]

Abstract

The quantification of the rate-of-rise of the thermal stratification interface, a "thin" vertical zone where the temperature gradient is the steepest, is important in assessing the potential implications of thermally-induced stress problems in liquid-metal cooled reactors. Thermal stratification can likewise occur in confined volumes containing ordinary fluids (Pr≥1), where there is an input of thermal convective energy. In the prominent case of liquid metal reactors, there have been many studies on quantifying the rate-of-rise of a defined stratification interface, in terms of one or more of the following dimensionless groups, mainly: Richardson (Ri), Reynolds (Re), Grashof (Gr), Rayleigh (Ra) and/or Froude (Fr) numbers. Stratification is also a transient process in the volume in question. In the present work the authors presents a derivation based on order-of-magnitude analysis (OMA), including an sensible energy balance, that produces a new representation more consistent than past studies. The representaion is shown to work well for past results. Furthermore, the representation is shown to be consistent with OMA of the conservation equations for natural, mixed and forced convection problems. Some fine points and aspects of OMA and the results are described.

[1] JNC International Fellow, Reactor Engineering Group, Oarai Engineering Center
[2] Reactor Engineering Group, Oarai Engineering Center

炉容器プレナム内での温度成層界面の上昇速度に関する検討（研究報告書）

Akira TOKUHIRO[1], 木村　暢之[2]

要旨

液体金属冷却高速炉（LMFBR）において、温度成層界面（軸方向温度勾配が最も急峻となる軸方向位置）の上昇速度を定量化することは、構造材への熱荷重を評価する上で重要である。温度成層化現象は、対流による生成エネルギーの入力がある Pr>1 の密閉空間内流体においても同様に発生する。LMFBR の温度成層化現象に関しては、成層界面の上昇速度を無次元数群（Ri、Rc、Gr、Ra[Fr]）により定量化する研究が数多く行われている。温度成層化現象は、炉容器プレナム内での過渡事象である。本研究では、エネルギーバランスを考慮に入れた概略解析（order-of-magnitude analysis; OMA）に基づく成層界面上昇速度の整理を行い、既往試験結果が１つの整理式によってまとめられることを示した。さらに、本整理は、自然／共存／強制対流問題における保存式の OMA と整合がとれていることを確認した。

1 大洗工学センター、ナトリウム・安全工学試験部、原子炉工学グループ
国際特別研究員
2 大洗工学センター、ナトリウム・安全工学試験部、原子炉工学グループ

List of Tables

List of Figures

1. Introduction

Thermal stratification phenomena in pool-type nuclear reactors, especially in liquid-metal cooled types in contrast to water-cooled, is of concern as an safety issue because fluid-solid interaction may cause thermal stress and fatigue of reactor components and materials. Thus in the design of the liquid-metal fast reactor (LMFR), the occurrence of thermal stratification must be well-understood. The topic was already recognized as being important in the late 1970s and early 1980s by Yang[(1)], Jones[(2)], Harrell[(3)], Carbajo[(4)], Howard and Carbajo[(5)], Carbajo and Howard[(6)], Vidil et al.[(7)], Grand et al.[(8)], Vidil et al.[(9)], Tanimoto et al.[(10)], Moriya et al.[(11)], Vidil et al.[(12)]. These early investigations were conducted as part of the American and French LMFR programs and established most of the phenomenological facts regarding thermal stratification in the reactor plenum. That is, the upper plenum gradually (time-wise) becomes thermally stratified due to input of thermal energy (convective flow) from flow out of the core and output of energy through, for example the intermediate heat exchanger. In subsequent years, similar experiments with regard to the Japanese LMFR program were conducted by Tanaka et al.[(13)] and Ieda et al.[(14)]. In recent years, emphasis has shifted to the numerical simulation of thermal stratification, including development of the appropriate turbulence model for simulation. One work in this areas is that by Muramatsu and Ninokata[(15)]. The latest of the sodium experiments in this context is that conducted by Kimura et al.[(16)].

In the present work we focus our attention to the works by Tanaka et al., Ieda et al., and Kimura et al., and specifically to the last work since it contains the data of the former and raises again, the question of the appropriate representation of the rate-of-rise of the thermally stratified interface in a finite volume with energy input. The rate-of-rise of the interface, though identified as relevant and quantified through measurement, has eluded a formal derivation from the conservation equations. This abbreviated work aims to present this derivation. Given such a derivation, it is then possible to compare the rate-of-stratification from various works in an uniform manner. Additionally, we aim to present a correlation describing the rate-of-rise in terms of familiar dimensionless groups. This is of course of importance to various system codes that simulate stratification and the consequences of stratification phenomena.

As for the validity and usefulness of order-of-magnitude analysis, it has been particularly well documented by Lykoudis[(17-19)], Lykoudis and Tokuhiro[(20)], Bejan[(21)] and several others. The method is for example used by Tennekes and Lumley[(22)]. This algebraic method of analysis of the conservation equations (in accepted differential equation form), gives all of the proper relationships traditionally accepted (and taken for granted) in heat transfer analysis, for example the relationship between Nusselt number (Nu) and Rayeigh number (Ra) in natural convection from a vertical plate in an infinite medium of Prandtl number, $Pr \geq 1$[1]. The method does have its limitations, just like more sophisticated mathematical methods. OMA inherently incorporates

[1] that is $Nu \sim (H/\delta) \sim Ra^{1/4}$ where $Ra \equiv g\beta\Delta T/\nu\alpha$

physically-based and intuitive arguments that are not so easily seen for example in complicated turbulence models. Finally, since the presented analysis is aimed toward liquid-metal cooled (nuclear) reactors, we use the term "ordinary fluids" to mean fluids for which Pr≥1 (water, oils), as opposed to liquid metals, for which Pr<1 (Pr<<1).

2. Analysis

2.1 Recasting of previous data

In their investigation on stratification phenomena in fast reactors, Kimura et al. plotted the dimensionless rate-of-rise of the thermal stratification interface (hereafter referred to as rate-of-rise), $(dH/dt)/V_t$, versus the Richardson (Ri) number and also the grouping, (Gr/Re). The stratification interface was designated as H. A comparison was made between their data in the scaled PLANDTL-DHX facility and that by Ieda et al. in sodium (1/10th scale), Tanaka et al. in water (CRIEPI) and Tanimoto et al. in water (MHI). The normalization velocity used in the presentation of data was, V_t, the core area averaged velocity out of the core. This choice of velocity is presented as the "natural" velocity scale for non-dimensionalizing the rate-of-rise of the interface. These figures are reproduced as **Figures 1** and **2**. We note that both plots show scatter of data points over several decades (log-log plot). In fact, contrary to the discussion presented by Kimura et al. a trend in the datum points is slightly more apparent in Fig. 1 than 2. We also note that the abscissal representation by the Ri-number, $Ri=(Gr/Re^2)$, is preferred because it is traditionally the parameter associated with mixed convection problems [Lloyd and Sparrow[23]] and indeed, expresses the ratio of buoyancy to inertial forces. In contrast, the (Gr/Re) grouping provides no such interpretation of a balance of forces. We also note that the CEA data[7-9,12] , although not shown, have the same slope as the data sets shown, but in a Ri-umber range, 7<Ri<70. In fact, the rate-of-rise of the interface, non-dimensionalized by the characteristic velocity of the "wall-jet", V_r, and using the ratio of the enclosure length to characteristic width of the "wall-jet", $L/x_{0.5}$, is,

$$\frac{V_i}{V_r}\frac{L}{x_{0.5}} = 0.37(Ri)_i^{-0.73} \qquad (1)$$

Ri_i is the local Ri-number at the interface. The "wall-jet" describes the horizontal jet flowing into the enclosed volume that modifies the stratification in the volume itself.

Bejan has however suggested and in fact demonstrates, for mixed convection of ordinary fluids and liquid metals respectively, that the proper dimensionless parameter is not Ri, but the ratio below, that is

$$\frac{Ra^{1/4}}{Re^{1/2}\cdot Pr^{1/3}} \text{ and } \frac{Bo^{1/4}}{Pe^{1/2}}. \qquad (2)$$

where to those unfamiliar, Bo and Pe are respectively the Boussinesq and Peclet numbers. This ratio stems from the fact that heat convects through the boundary layer,

thermal (δ_{th}) or momentum (δ_{mom}), whichever is thinner (smaller) in mixed convective situations and for example in ordinary fluids, we know that δ_{mom}~$HRe^{1/2}Pr^{1/3}$ and δ_{th}~$HRa^{1/4}$. There is an equivalent relationship low Prandtl number fluids. Also recall that the Bo-number is the proper dimensionless number for natural convection in low Prandtl number fluids, [Lykoudis and Tokuhiro[20], Bejan[21]]. It is related to the Grashof and Prandtl numbers by the relationships,

$$Bo^{"} = Gr^{*}\,\mathrm{Pr}^{2}; Bo = Gr\,\mathrm{Pr}^{2} \tag{3}$$

Equation (1) is for mixed convection in an idealized infinite medium. In the present case, though large in extent, the plenum can be considered a finite enclosure of height (H) and length (L) so that the aspect ratio is (H/L). The particular enclosure within the realm of fast reactors is, in this case the upper plenum (see **Fig. 3**), and features flow from the core that impinges on the UIS and enters the upper plenum at the edge of the UIS. Thus calling upon results from **Appendix B** for natural convection in an *enclosure*, instead of (1) we have,

$$\frac{Ra^{2/7}\left(\frac{H}{L}\right)^{1/7}}{\mathrm{Re}^{1/2}\cdot\mathrm{Pr}^{1/3}} \text{ and } \frac{Bo^{2/7}\left(\frac{H}{L}\right)^{1/7}}{Pe^{1/2}} \tag{4}$$

When we recast these two in terms of the Grashof, Richardson and Prandtl numbers, we arrive with the grouping, $(Ri^{1/4}Gr^{1/28}(H/L)^{1/7})Pr^{1/14}$ for Pr<<1 and $(Ri^{1/4}Gr^{1/28}(H/L)^{1/7})Pr^{-1/21}$ for Pr≥1. Here we must remember that the $Ri^{1/4}$ itself contains the Gr-number so that the $Gr^{1/28}$ is not a reflection of the weak dependency on Gr. In contrast however, the Pr-number dependence for Pr<<1 is stronger than that for Pr≥1; that is, a one order change in Pr-number (0.1 to 0.01) gives a 15% change relative to a 0.78% change for ordinary fluids (1 to 10).

Upon replotting Figs. 1 and 2 using the grouping (3), the datum points plotted over the same number of decades collapse as shown in **Figure 4**. The corresponding correlation, based on a linear regression through the data is,

$$\frac{(dH/dt)}{V_t} = 0.0493\left[\mathrm{Ri}^{1/4}\mathrm{Gr}^{1/28}(\mathrm{H}/\mathrm{L})^{1/7}\mathrm{Pr}^{1/14}\right]^{0.0015} \tag{5}$$

where we have chosen the relatively more "sensitive" $Pr^{1/14}$-dependence. The representation is apparently correct, as it accounts for both ordinary fluids and liquid metals. In addition as Bejan notes on the correctness of dimensionless data presentation, approximately all the points fall within one order-of-magnitude along the ordinate and abscissa.

There are a few points of contention, one being the appropriate definition for the average velocity of flow into the upper plenum, V_t . Since it is not clear how this velocity should be calculated or estimated, there is an uncertainty associated with comparison of various experimental results. At the same time one expects that the

rate-of-rise of the interface should be amenable to simple analysis, such as an energy balance of convective to conductive heat transfer into a defined enclosure. In fact, the stratification phenomena in the upper plenum (or in an enclosure) should contain parameters describing the properties (dimensions, thermal properties) of the enclosure. We will thus explore these possibilities in the section to follow.

2.2 Derivation of the rate-of-rise from first principles

Consider the control volume in which the rate-of-rise of the stratification interface occurs. That is, essentially the flow convected horizontally from the region of the UIS/UCS into the upper plenum at a characteristic velocity, U_x. This is shown in **Figure 3**. The associated characteristic temperature difference in and out of the core (that determines U_x) is, ΔT_{i-o} ($=T_O-T_i$), and the quasi-stagnant upper plenum, described by an overall thermal conductivity, k_x, spans vertically and in width, X and L, respectively. The vertical temperature difference due to stratification is ΔT_S ($=T_H-T_O$). The vertical span X is also the height over which this boundary later approximation is valid, while the third dimension is considered to be of unit depth. The thermal physical properties, ρ and C_p are that associated with the flow, U_x. If we consider a energy balance between the thermally convected energy and conduction in the stratified plenum we have,

$$\rho C_P \Delta T_{i-o} U_x \delta(1) \sim k_x \frac{\Delta T_S}{X} L(1) \tag{6}$$

Next, consider for the moment that stratification is driven by natural convection. We can then call upon an order-of-magnitude analysis of the energy equation, for natural convection in an enclosure. Details are shown in Appendix A (specifically equation A-2). This provides us with one of two interpretations of U_x; that is, from the energy equation we get that $U_x \sim \alpha X/\delta^2$. Using this then gives, when substituted into (5) with $\Delta T_{i-O} \sim \Delta T_S$, that

$$X \sim \sqrt{\delta L}\ . \tag{7}$$

Equally instead of associating U_x with the flow from the core, if we then think of this characteristic velocity as that describing the rate-of-rise of the stratification interface, we have that $U_x \sim (dX/dt)$ so that,

$$\rho C_P \Delta T_{i-o} \frac{dX}{dt} \delta(1) \sim k_x \frac{\Delta T_S}{X} L(1) \tag{8}$$

or solving for dX/dt gives,

$$\frac{dX}{dt} \sim \frac{\alpha}{X} \frac{\Delta T_S}{\Delta T_{i-o}} \frac{H}{\delta} \frac{L}{H} \tag{9}$$

Then using (7) we change it to,

$$\frac{dX}{dt} \sim \frac{\alpha}{H}\frac{\Delta T_S}{\Delta T_{i-o}}\frac{H}{\delta}\frac{L}{\delta^{1/2}L^{1/2}} \tag{10}$$

Given this form we have unified the region of relevance of the thermal properties to that pertaining to the upper plenum only; that is, we implicitly assume that the thermal properties associated with the convective flow is not too different from the thermal conductivity of the "core" of the upper plenum.

From equation (8) we use the heat transfer relationships for liquid metals and ordinary fluids, each separately considered for a natural or forced convection driven change in the thermal stratification. So, using first the results from Appendix A, we get the following expression for the rate-of-rise of the stratification interface instead of the previous equation; that is,

$$\frac{\left(dX/dt\right)}{\left(\alpha/H\right)} \sim \frac{\Delta T_S}{\Delta T_{i-o}} Bo^{3/7}\left(\frac{L}{H}\right)^{2/7} \tag{11}$$

By analogy for a ordinary fluid, we get

$$\frac{\left(dX/dt\right)}{\left(\alpha/H\right)} \sim \frac{\Delta T_S}{\Delta T_{i-o}} Ra^{3/7}\left(\frac{L}{H}\right)^{2/7} \tag{12}$$

We note here that the rate-of-rise is contrary to Fig. 4, is now non-dimensionalized by the (α/H) which describes not only the height of the enclosure, but also its thermal diffusivity. There is also the ratio, ($\Delta T_s/\Delta T_{i-o}$), which describes the temperature difference due to stratification and that driving the stratification.

For forced convection, we have for a liquid metal and ordinary fluid, respectively

$$\frac{\left(dX/dt\right)}{\left(\alpha/H\right)} \sim \frac{\Delta T_S}{\Delta T_{i-o}} Pe^{3/4}\left(\frac{L}{H}\right)^{1/2} \tag{13}$$

and

$$\frac{\left(dX/dt\right)}{\left(\alpha/H\right)} \sim \frac{\Delta T_S}{\Delta T_{i-o}} \mathrm{Re}^{3/4}\,\mathrm{Pr}^{1/2}\left(\frac{L}{H}\right)^{1/2} \tag{14}$$

The ratio thus expresses a mixed convective flow and assuming $\Delta T_{i\text{-}o} \sim \Delta T_S$, we have that

$$\frac{\left(dX/dt\right)}{\left(\alpha/H\right)} \sim \frac{Bo^{3/7}}{Pe^{3/4}}\left(\frac{H}{L}\right)^{3/14} \tag{15}$$

By analogy for a ordinary fluid, we get

$$\frac{\left(dX/dt\right)}{\left(\alpha/H\right)} \sim \frac{Ra^{3/7}}{\mathrm{Re}^{3/4}\,\mathrm{Pr}^{1/2}}\left(\frac{H}{L}\right)^{3/14} \tag{16}$$

Two details warrant a few comments. First with do not exactly know the nature of the convection that drives the stratification; that is, we do not explicitly know whether the heat transfer at the "interface" occurs at constant heat flux, constant temperature, a combination of the two or by other means. By interface we mean the approximate region that separates what is thermally stratified and across which convective exchange takes place. We do know that constant temperature and heat flux present two limiting cases.

Secondly, we have assumed $\Delta T_{i\text{-}o} \sim \Delta T_S$ as mentioned. In analogy to natural convection in an enclosure, which in fact becomes slowly (thermal) stratified, the temperature difference across the boundary layer, ΔT_W , and that describing stratification, ΔT_S , in most cases is nearly the same; that is, of order O~1. However, as Uotani[24] and Lykoudis and Tokuhiro[20] showed, this equivalency in magnitude does not exactly hold for liquid metals. That is, physically because of the large thermal diffusivity relative to the convective heat input, stratification can be substantial in the volume enclosing a liquid metal. So, a correction in order to account for the ratio, $\frac{\Delta T_S}{\Delta T_{i-o}}$, is needed especially when comparing stratification data of liquid metals versus ordinary fluids.

3. Discussion

The recasting of data from Figs. 1 and 2, in terms of Bejan's mixed convection parameter is shown to work well in Fig. 4. We however, present in **Figure 5** a plot of the rate-of-rise of the stratification interface, described by (dX/dt), and non-dimensionalized by the rate-of-diffusion through a medium of vertical extent, H, and thermal diffusivity α. The relationships used are for natural convection in an infinite medium (simply "natural convection" in Table 1) and forced convection (both laminar). Note that since ordinate "x-axis" expresses a ratio of natural to forced convective dimensionless groups, the "y-axis" must be consistently represented. The x- and y-coordinate scales are derived from Eq. (10) and the appropriate relationships in Table 1. The y-axis of course shows the grouping for respectively liquid metal and

ordinary fluids. As evident, although the trend is expectedly linear, there is slightly more scatter amongst the data than the previous figure. Since the previous figure also used laminar relationships, the scatter here may be an indication of the lack of accounting of the aspect ratio (H/L) of the enclosure geometry.

Thus in **Figure 6** we depict the data according to Eqs. (13) and (14) for liquid metals and ordinary fluids respectively, where the aspect ratio is included. That is, in contrast to Fig. 6, we have used the relationship here for natural convection in an enclosure. Here the datum points clearly distinguish between liquid metals and ordinary fluids. The linearity is however, similar for the two types of liquids. The only difference between Pr<<1 and Pr ≥ 1, is the relative ratio of magnitudes of the characteristic temperature differences, due to stratification and that between the core inlet-and-outlet; that is, $\frac{\Delta T_S}{\Delta T_{i-o}} = \frac{T_H - T_0}{T_i - T_0}$ where T_H, T_i and T_O respectively represent the bulk temperature at elevation H and temperatures in and out of the reactor core. The latter is not a strict definition, but should describe the characteristic temperature that "drives" the stratification interface.

If we thus account for the temperature ratio above and incorporate it in our sodium data, we arrive at **Figure 7**. In order to account for $\frac{\Delta T_S}{\Delta T_{i-o}}$, we impose a balance between the conductive and convective heat fluxes and assume that the length scale of each heat transfer mode is equal. Here again the two data sets have similar linearity, but also a slight difference with respect to the coordinates. It is difficult to attribute this small difference to any unaccounted for physical phenomena. Equally, we recognize the limits of simplified analysis. We thus recommended a single linear regression line through all of the data and note that it is given by, $Y=1.685X^{-2.215}$ where X and Y are respectively the "new" groupings shown along the abscissa and ordinate. The coefficient of correlation is 0.75.

For completeness we also include in **Figure 8** the rate-of-rise of the interface plotted in terms of the traditionally cited functional dependencies for forced turbulent convection, for both ordinary fluids and liquid metals. The correlation used for ordinary fluids is the often cited Dittus-Boelter correlation, which has a $hD/k \sim Pr^{0.4} Re_D^{0.8}$ dependency. The characteristic length in this case, D, is the diameter of the duct. Equally, for liquid metals we use the correlation suggested by Sleicher and Rouse[25] given as $hD/k \sim Re_D^{0.85} Pr^{0.93}$, but simplify it to $Pe_D^{0.85}$(Pe=RePr), by neglecting the small decimal difference in the Re- and Pr-number exponents. One can see that similarly to Fig. 6, the data sets are divided along the types of fluids, but the points are clustered closer together in contrast to Fig. 6.

Since the functional dependency for water and sodium are similar (slope of the trend for each) and we would like to propose a single correlation, we note that sodium datum points can be viewed as being displaced from the water data by a constant. We also note that the correlation of Sleicher and Rouse contains a constant. We thus insert a constant, "6.6", to our sodium data and suggest the following correlation for all the data points. The correlation shown in **Figure 9** is,

$$\frac{(dX/dt)}{(\alpha/H)(L/H)^{1/2}\,Pe^{0.85}} = 97.665\left(\frac{Bo^{1/3}(H/L)^{3/14}}{Pe^{0.85}}\right)^{-2.505} \tag{17}$$

or equally,

$$\frac{(dX/dt)}{(\alpha/H)(L/H)^{1/2}\,\mathrm{Re}^{0.80}\,\mathrm{Pr}^{0.40}} = 97.665\left(\frac{Ra^{1/3}(H/L)^{3/14}}{\mathrm{Re}^{0.80}\,\mathrm{Pr}^{0.40}}\right)^{-2.505} \tag{18}$$

since the Bo- and Pe-number should be used for liquid metals and Ra-, Re- and Pr-numbers for ordinaty fluids. The correlation of coefficient of 0.72, while the validity of the correlation is *limited to* the scale shown in the figure.

4. Conclusions

Knowledge of the rate-of-rise of the thermal stratification interface in the upper plenum of many liquid-metal cooled pool-type reactors is important because the dynamic movement of this "thin" vertical zone where the temperature gradient is the steepest, influences thermally-induced stress problems during life-cycle of the reactor.

Thermal stratification can likewise occur in confined volumes containing ordinary fluids (Pr≥1), where there is an input of thermal convective energy. In the prominent case of liquid metal reactors, there have been many studies on quantifying the rate-of-rise of a defined stratification interface, in terms of one or more of the following dimensionless groups, mainly: Richardson (Ri), Reynolds (Re), Grashof (Gr), Rayleigh (Ra) and/or Froude (Fr) numbers. Stratification is also a transient process in the volume in question. In the present work the authors presents a derivation based on order-of-magnitude analysis (OMA), including an sensible energy balance, that produces a new representation more consistent than past studies. The representation is shown to work well for past results. Furthermore, the representation is shown to be consistent with OMA of the conservation equations for natural, mixed and forced convection problems. A correlation is proposed based on the available data pertaining to the rate-of-rise of the stratification interface.

Appendix A:

The mixed convection parameter according to Bejan.

To arrive at this Bejan[21] grouping for mixed convection who first noted that a region of higher temperature seeks the nearest heat sink. Thus the transition from natural to forced convection is governed by the smaller (thinner) of the thermal boundary layers originating from natural convection (NC) or forced convection (FC). So, if

$$(\delta_T)_{NC} < (\delta_T)_{FC}, \text{ then natural convection dominates} \tag{A1}$$

$$(\delta_T)_{NC} > (\delta_T)_{FC}, \text{ then forced convection dominates} \tag{A2}$$

Thus respectively for ordinary fluids, Pr≥1 (OFs), and liquid metals, Pr<1 (LMs), since we know that,

$$(\delta_T)_{NC,OFs} \sim H\,Ra^{1/4}, (\delta_T)_{FC,\,OFs} \sim H\,Re^{1/2}\,Pr^{1/3} \tag{A3}$$

$$(\delta_T)_{NC,LMs} \sim H\,Bo^{1/4}, (\delta_T)_{FC,\,LMs} \sim H\,Pe^{1/2} \tag{A4}$$

the proper ratio for mixed convection and thus the dimensionless grouping is,

$$\frac{Ra^{1/4}}{Re^{1/2}\cdot Pr^{1/3}} > O(1), \text{ natural convection; } < O(1), \text{ forced convection} \tag{A5}$$

$$\frac{Bo^{1/4}}{Pe^{1/2}}\{ > O(1), \text{ natural convection; } < O(1), \text{ forced convection} \tag{A6}$$

where in the latter, Bo and Pe, are respectively the Boussinesq and Peclet numbers.

Bejan notes that the Ri-number is in fact,

$$Ri \equiv \frac{Gr}{Re^2} = \left(\frac{Ra^{1/4}}{Re^{1/2}\cdot Pr^{1/3}}\right)^4 Pr^{1/3} \tag{A7}$$

Thus plotting $\frac{Nu}{Re^{1/2}\,Pr^{1/3}}$ versus $\frac{Ra^{1/4}}{Re^{1/2}\cdot Pr^{1/3}}$ instead of Nu versus Ri, Bejan has shown that instead of three curves, one each for Prandtl numbers Pr=0.72, 10 and 100 , these trends collapse onto one line [see Bejan, Fig. 4.12 and 4.13].

Appendix B:

Natural convection in a rectangular enclosure with aspect ratio $\left(\frac{H}{L}\right)$ (vice versa).

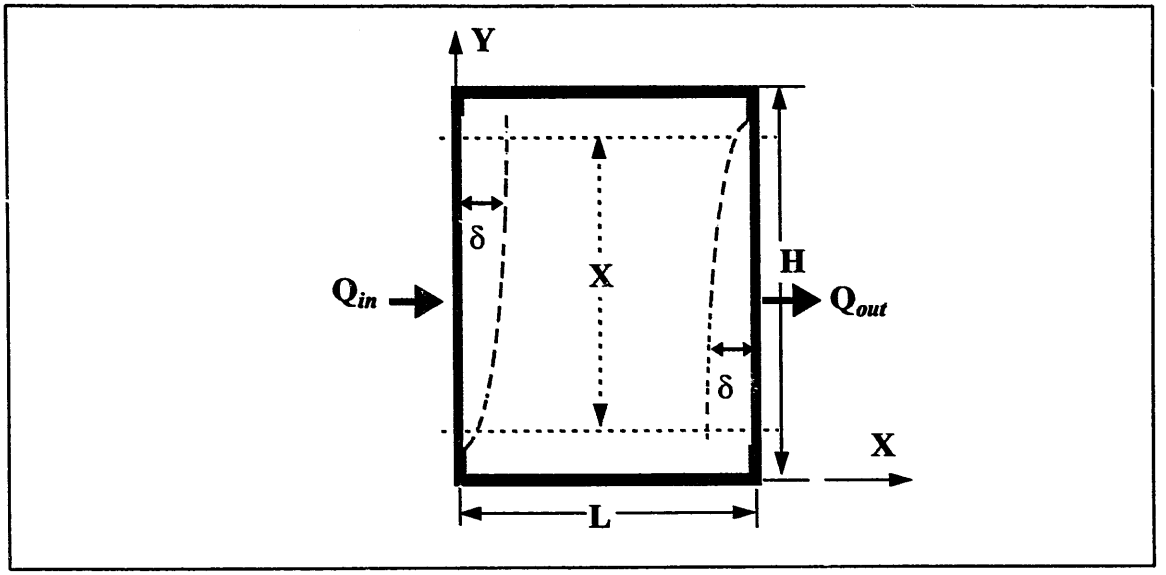

Figure B1. Schematic of natural convection in an rectangular enclosure with aspect ratio (H/L).

Consider natural convection in an enclosure of aspect ratio, (H/L) or vice-versa, with adiabatic walls at the top and bottom and heat input/output, Q_{in} and Q_{out}, at the left and right walls respectively as shown above. The momentum and/or thermal boundary layer thickness at each wall is δ and the vertical distance X, defines the height along which the boundary layer approximation is valid. We address the case for a liquid metal first, wherein the momentum equation expresses a balance between the inertial and buoyancy forces. So, the momentum and energy equations give,

Momentum:
$$\frac{U^2}{X} \sim g\beta\Delta T \tag{B1}$$

Energy:
$$\frac{U\Delta T}{X} \sim \frac{\alpha\Delta T_X}{\delta^2} \tag{B2}$$

The height X is fixed by saying that the amount of energy convected upwards is equal to the amount that is conducted in the core along X. Thus,

$$\rho c_P \Delta T U_y \delta(1) \sim k_X \frac{\Delta T_X}{X} L(1) \tag{B3}$$

$$U_y \delta \sim \frac{\alpha_X}{X} L \tag{B4}$$

Substituting for U_y from Eq. [2], taking $\Delta T \sim \Delta T_X$, gives

$$X = \sqrt{\delta L} \tag{B5}$$

From here proceed as usual as if X=H; that is, substituting for U in the momentum equation, from the energy equation, gives,

$$\left(\frac{X}{\delta}\right)^4 \sim \frac{g\beta\Delta T X^3}{\alpha^2} \tag{B6}$$

Realizing that one wants an expression in terms of $\left(\frac{H}{\delta}\right)$ and noting that $q" = k\frac{\Delta T}{\delta}$ gives after a bit of algebra,

$$Nu \sim \left(\frac{H}{\delta}\right) \sim Bo^{*2/9} \left(\frac{H}{L}\right)^{1/9} \tag{B7}$$

for Pr<<1, $q"$=constant heat flux at the wall, and

$$Nu \sim \left(\frac{H}{\delta}\right) \sim Bo^{2/7} \left(\frac{H}{L}\right)^{1/7} \tag{B8}$$

for Pr<<1, T_w=constant temperature at the wall. The Boussinesq number is defined as, $Bo = \frac{g\beta\Delta T L^3}{\alpha^2}$, and as noted in our work and that by Bejan [Cf.] is the appropriate one for low Prandtl number fluids.

For ordinary fluids, Pr≥1, including air and water, we get the equivalent results as follows,

$$Nu \sim \left(\frac{H}{\delta}\right) \sim Ra^{*2/9} \left(\frac{H}{L}\right)^{1/9} \tag{B9}$$

for Pr≥1, $q"$=constant heat flux at the wall, and

$$Nu \sim \left(\frac{H}{\delta}\right) \sim Ra^{2/7} \left(\frac{H}{L}\right)^{1/7} \tag{B10}$$

for Pr≥1, T_w=constant temperature at the wall. Here the Rayleigh number is defined as, $Ra = \frac{g\beta\Delta T L^3}{\alpha\nu}$.

Appendix C:

Definitions of dimensionless groups and variables from past studies

CEA[sodium]: $Ri \equiv g\beta\Delta TL/V_0^2$

$Re \equiv V_0 L/\nu_0$

V_0-average velocity in the test section inlet channel

"[ ]" indicate test medium

PNC/JNC[sodium]:

$Ri \equiv g\beta\Delta TL/V_0^2$

$Re \equiv V_0 L/\nu_0$

V_0-average velocity in the test section inlet channel

CRIEPI[water]:

$Ri \equiv (\pi/4)^2 (\rho_c - \rho_h/\rho_c)\, g\, D^5/Q^2$

$Re \equiv (4/\pi)Q/D\nu$

Q-volumetric flowrate

MHI[water]:

$Ri \equiv g\beta\Delta TL/V_0^2$

$Re \equiv V_0 L/\nu_0$

V_0-average velocity in the test section inlet channel

Nomenclature

Bo, Bo*: Boussinesq number at constant temperature and heat flux, = $(g\beta\Delta TH^3/\alpha^2)$, = $(g\beta q"H^4/\alpha^2 k)$

C_p : heat capacity at constant pressure, [J/kgK]

Fr: Froude number, =($g\beta\Delta TH/U^2$)

Gr, Gr*: Grashof number, = $(g\beta\Delta TH^3/\nu^2)$, = $(g\beta q"H^4/\nu^2 k)$

H, (H/L): vertical length of enclosure, aspect ratio of enclosure

(dH/dt) : rate-of-rise of the stratification interface

k_x : thermal conductivity along x-direction, [W/mK]

L, (L/H) :horizontal length of enclosure, inverse aspect ratio of enclosure

OMA: Order of Magnitude Analysis

Pe: Peclet number, =(UL/α)

Pr: Prandtl number, =(ν/α)

$q"$: heat flux, [W/m^2]

Q_{in}, Q_{out} : heat in and out of the enclosure in Fig. B1

Ra, Ra* : Rayleigh number, = $(g\beta\Delta TH^3/\alpha\nu)$, =($g\beta q"H^4/\alpha\nu k$),

Re: Reynolds number of inlet channel, = (UD/ν) or (Uz/ν)

Ri: Richardson number, = (Gr/Re^2)

ΔT_S , ΔT_{i-o} , ΔT_X: temperature difference describing the stratification, difference in temperature in and out of the core, temperature difference along the x-axis, [°C]

U, U_X, U_Y : characteristic velocity, characteristic velocity along the x-axis, [mm/s]

V_t : average velocity of flow into the upper plenum

X, Y: coordinate axes as in Fig. B1

Greek Symbols

α : thermal diffusivity, [m^2/s]

β: coefficient of thermal expansion, [1/K]

δ, δ_{th} , δ_{mom} : boundary layer thickness, thermal and momentum boundary layer thickness

$\rho_{cold,\ exit}$, $\rho_{hot,exit}$: Density of cold and hot jets, [kg/m^3]

Acknowledgments

The first author would like to thank Japan Nuclear Fuel Cycle Institute (formerly Power Reactor and Nuclear Fuel Development Corporation) for his appointment as JNC International Fellow. The author also thanks Mr. N. Kimura for providing the data contained in his publication and acknowledges the advice of Mr. M. Nishimura and H. Kamide.

References

(1) Yang, J.W., "Penetration of turbulent jet with negative buoyancy into the upper plenum of a LMFBR": *Nucl. Eng. Des.*, **40**, 297 (1977).

(2) Jones, P. "A study of transient buoyancy-induced flow stratification relevant to the primary pool of an LMFBR": *6th Int. Heat Transf. Conf.*, Toronto, Canada, Vol. 5, p. 137 (1978).

(3) Harrell, J. A., "Correlations for the rise rate of the hot-cold interface in a liquid metal fast breeder reactor": *MS Thesis, University of Illinois at Urbana-Champaign* (USA), May (1978).

(4) Carbajo, J. J., "Stratification criteria in LMFBR outlet plena": *Trans. Am. Nucl. Soc.*, **33**, 955 (1979).

(5) Howard, P.A. and J. J. Carbajo, J. J., "Experimental study of SCRAM transients in generalized liquid metal fast breeder reactor outlet plenum", *Nucl. Technol.*, **44**, 210 (1979).

(6) Carbajo, J. J. and Howard, P. A., "PLENUM-2A, a program for transient analysis of liquid-metal fast breeder reactor outlet plenum": *Nucl. Technol.*, **47**, 244 (1980).

(7) Vidil, R., Martin, R. and Grand, D., "Physical modeling of thermohydraulic phenomena in LMFBR": Nucl. React. Therm. Hydr. Top. Mtg., Saratoga, NY, USA (1980).

(8) Grand, D., *et al.* "Combined convection of sodium in a rectangular cavity": *Proc. Nucl. React. Therm. Hydr. Top. Mtg.*, Saratoga, NY, USA, (1980).

(9) Vidil, R., *et al.* "Experimental and numerical studies of mixed convection in a cavity. Case of sodium and water": *Proc. 7th Int. Heat Transf. Conf.*, Munich, Germany, 489 (1981).

(10) Tanimoto, K., *et al.* "Investigation of thermal stratification based on water experiments": *Atomic Energy Society of Japan, Fall Mtg.*, B51 (1986) [in Japanese].

(11) Moriya, S., *et al.* "Effects of Reynolds number and Richardson number on thermal stratification in hot plenum": *Nucl. Eng. and Des.*, **99** , 441(1987).

(12) Vidil, R., Grand, D. and Leroux, F., "Interaction of recirculation and stable stratification in a rectangular cavity filled with sodium": *Nucl. Eng. and Des.*, **105**, 321 (1988).

(13) Tanaka, N., *et al.* "Prediction method for thermal stratification in a reactor vessel": *Nucl. Eng. and Des.*, **120** , 395 (1990).

(14) Ieda, Y., *et al.* "Experimental and analytical studies of the thermal stratification phenomenon in the outlet plenum of fast breeder reactors": *Nucl. Eng. and Des.*, **120** 403 (1990).

(15) Muramatsu, T. and Ninokata, H., "Investigation of turbulence modeling in thermal stratification analysis": *Nucl. Eng. and Des.*, **150**, 81(1994).

(16) Kimura, N., *et al.* "An investigation of thermal stratification phenomena in fast reactors - sodium experiments and analyses - " : *Proc. 7th Int. Conf. Nucl. Eng. (ICONE-7)*, Tokyo, Japan, CD-RM (1999).

(17) Lykoudis, P.S. : "Non-dimensional numbers as ratios of characteristic times" Int. *J. Heat Mass Transf.* , **33**(**7**), 1568 (1990).

(18) Lykoudis, P.S. : "Introduction to the method of average magnitude analysis and application to natural convection in cavities", *ASME J. Heat Transf.*, **117**, 604 (Aug. 1995)

(19) Lykoudis, P.S. : "The Tau equations --- An alternative to Buckingham's Pi Theorem" Proc. 8th Int. Beer-Sheva Conf., AIAA publication to appear (1999).

(20) Lykoudis, P.S. and Tokuhiro, A. T., "Natural convection over a vertical heated flat plate with gas injection and in the presence of a magnetic field", AIAA, from *Proc. of the Mtg. on Turbulence and MHD*, Beer-Sheva, Israel, p. 601 (1992).

(21) Bejan, A.: *"Convection Heat Transfer"*, 1st ed., John Wiley and Sons, New York, USA, 142 (1984).

(22) Tennekes, H. and Lumley, J. L.: *"A First course on Turbulence"*, MIT Press, Cambridge, USA (1972).

(23) Lloyd and Sparrow, E. M. "Combined forced and free convection flow on vertical surfaces" : *Int. J. Heat Mass Transf.* , **13**, 434 (1970).

(24) Uotani, M. "Natural convection heat transfer in thermally stratified liquid metal": *J. Nucl. Sci. Technol.* , **24**(6) , 442 (1987).

(25) Sleicher, C.A. and Rouse, M. W., "A convenient correlation for heat transfer to constant and variable property fluids in turbulent pipe flow" : *Int. J. Heat Mass Transfer*, **18**, 677 (1975).

Table 1. Summary of relationships

Heat transfer Nu~(H/δ)	Ordinary Fluids Pr≥1	Liquid Metals Pr<1 (Pr<<1)	Notes
1) Natural convection	$Nu \sim Ra^{1/4}$	$Nu \sim Bo^{1/4}$	T_w=const.; OMA derivation in Bejan
2) Natural convection	$Nu \sim Ra^{*1/4}$	$Nu \sim Bo^{*1/4}$	q"=const.;
3) Natural convection enclosure, H/L	$Nu \sim Ra^{2/7}(H/L)^{1/7}$	$Nu \sim Bo^{2/7}(H/L)^{1/7}$	T_w=const.;
4) Natural convection enclosure, H/L	$Nu \sim Ra^{*2/9}(H/L)^{1/9}$	$Nu \sim Bo^{*2/9}(H/L)^{1/9}$	q"=const.
5) Mixed convection	$Nu \sim Ra^{1/4}/Re^{1/2}Pr^{1/3}$	$Nu \sim Bo^{1/4}/Pe^{1/2}$	not $Ri \equiv Gr/Re^2$
6) Rate-of-rise of TS-interface Kimura et al.	$(dX/dt)/V_t$ ~Ri and Gr/Re	$(dX/dt)/V_t$ ~Ri and Gr/Re	Figures 1 and 2
7) Rate-of-rise of TS-interface by nat. conv.	$(dX/dt)/(\alpha/H)$ $\sim(\Delta T_s/\Delta T_w)Ra^{3/7}(L/H)^{2/7}$	$(dX/dt)/(\alpha/H)$ $\sim(\Delta T_s/\Delta T_w)Bo^{3/7}(L/H)^{2/7}$	
8) Rate-of-rise of TS-interface by mixed conv.	$(dX/dt)/(\alpha/H)$ $\sim Ra^{5/7}(L/H)^{5/14}/Re^{5/4}\,Pr$	$(dX/dt)/(\alpha/H)$ $\sim Bo^{5/7}(L/H)^{5/14}/Pe^{5/4}$	

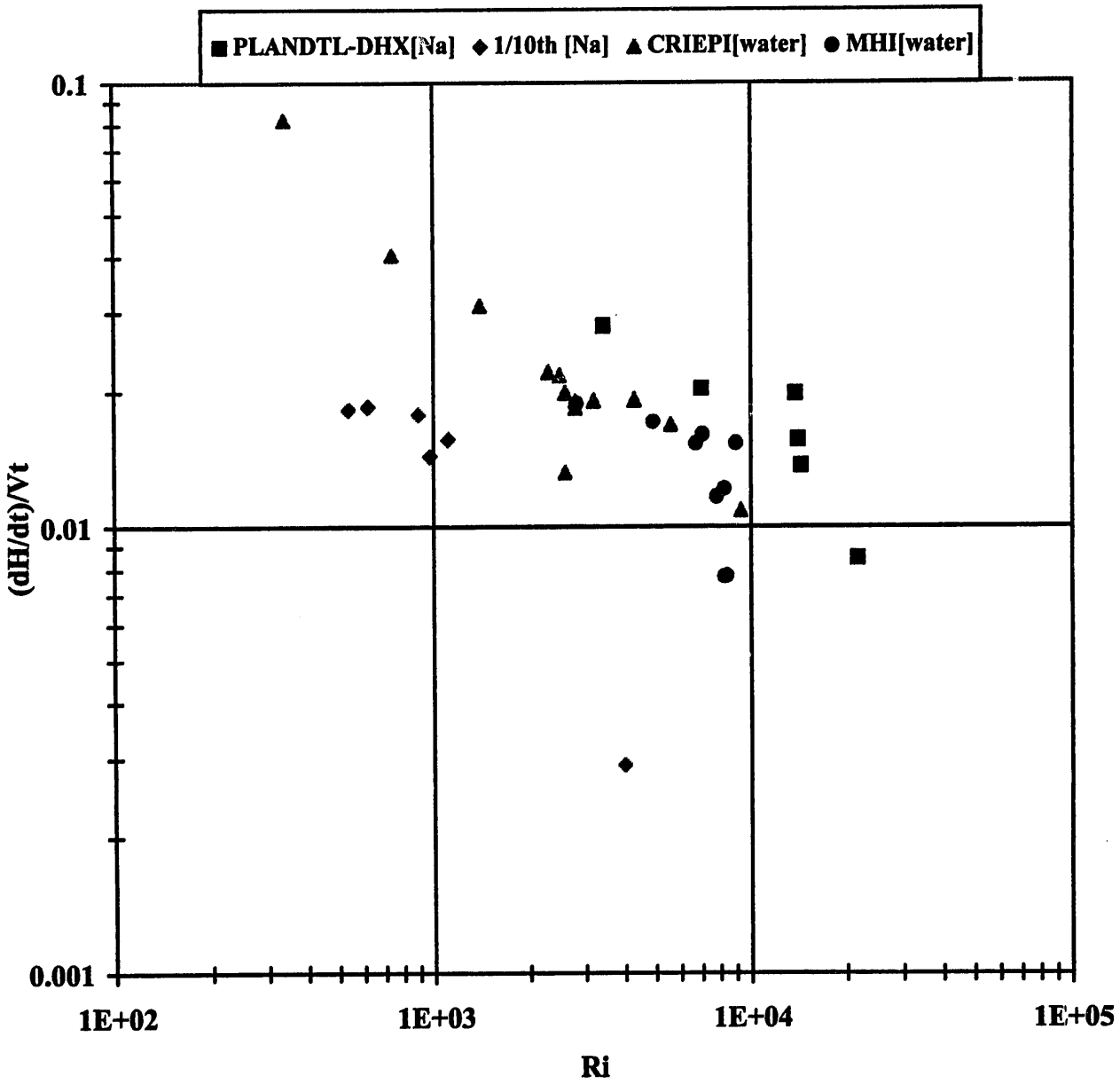

Figure 1. Rate-of-rise of defined stratification interface versus Ri-number.

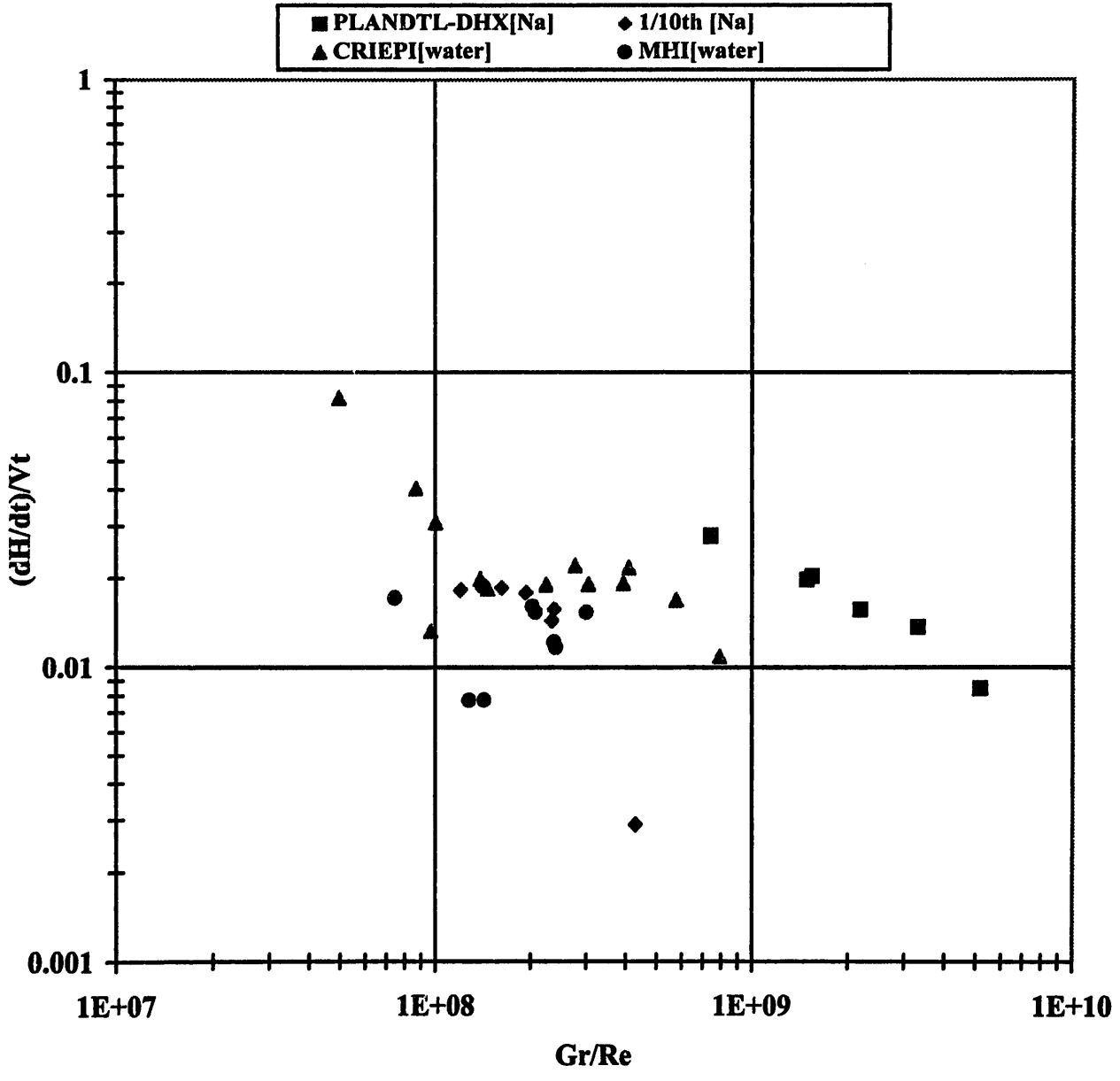

Figure 2. Rate-of-rise of defined stratification interface versus (Gr/Re).

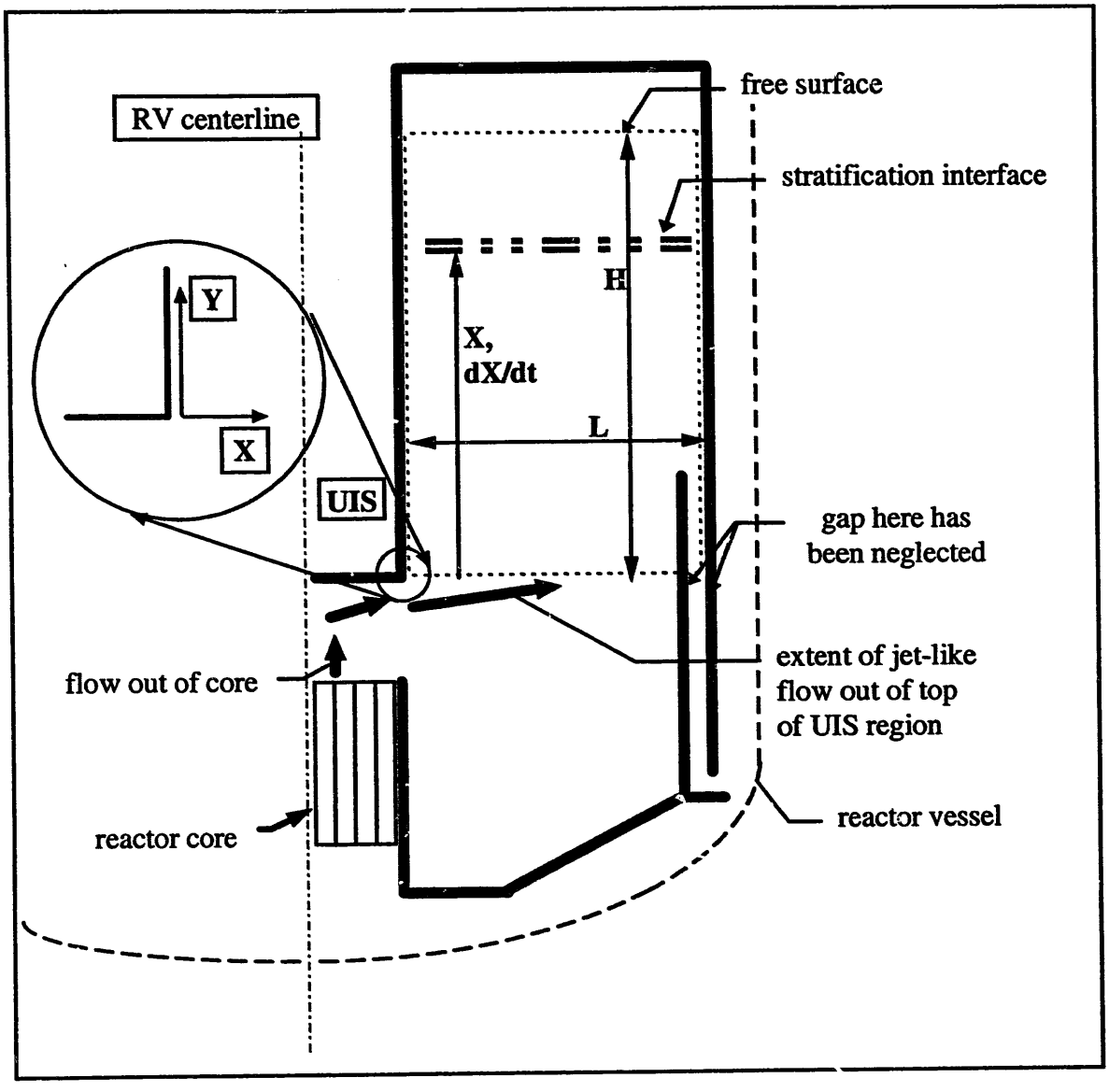

Figure 3. Schematic of upper plenum and relavant dimensions and parameters used in the analysis.

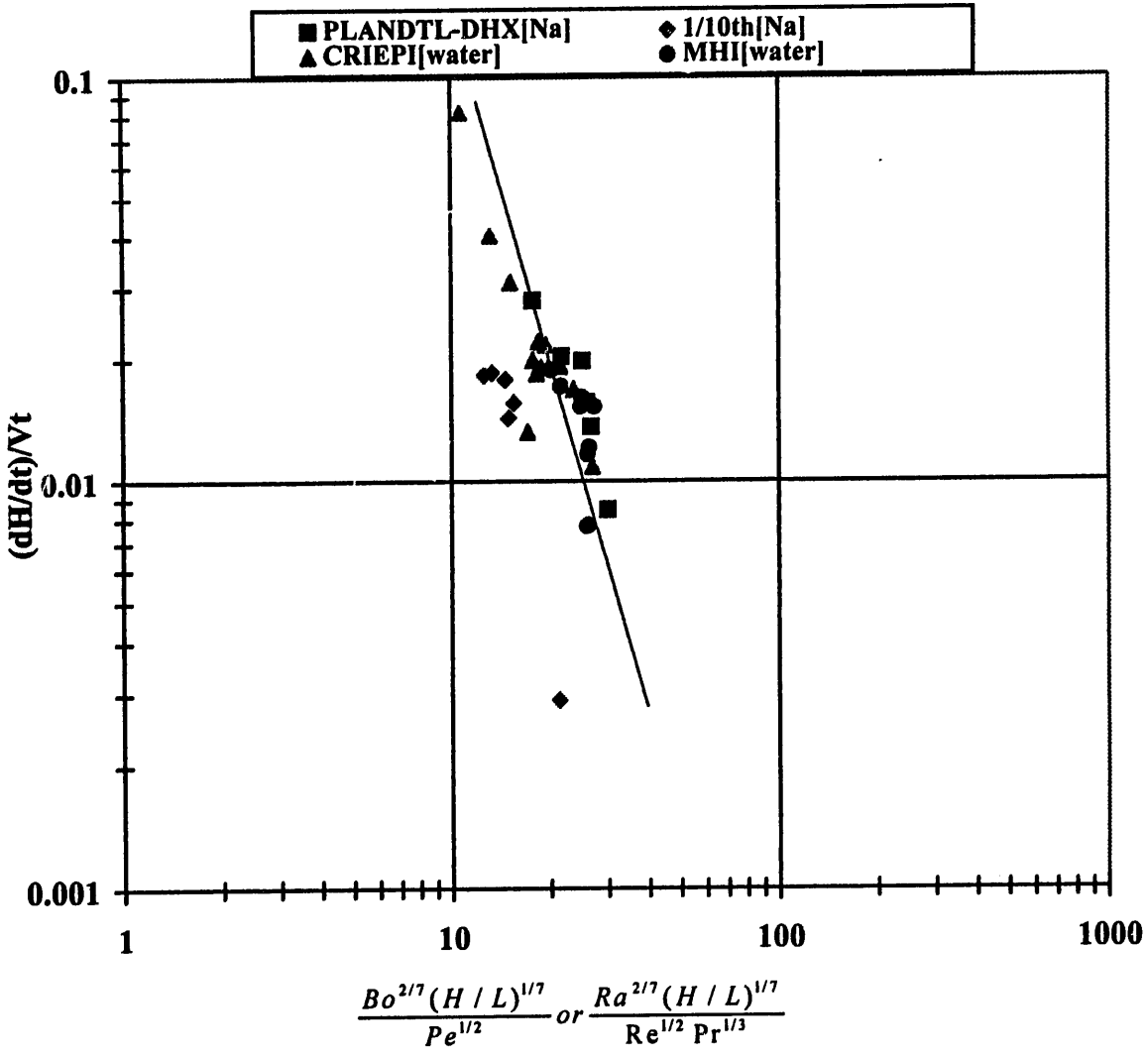

Figure 4. Rate-of-rise of defined stratification interface versus mixed convection in an enclosure grouping.

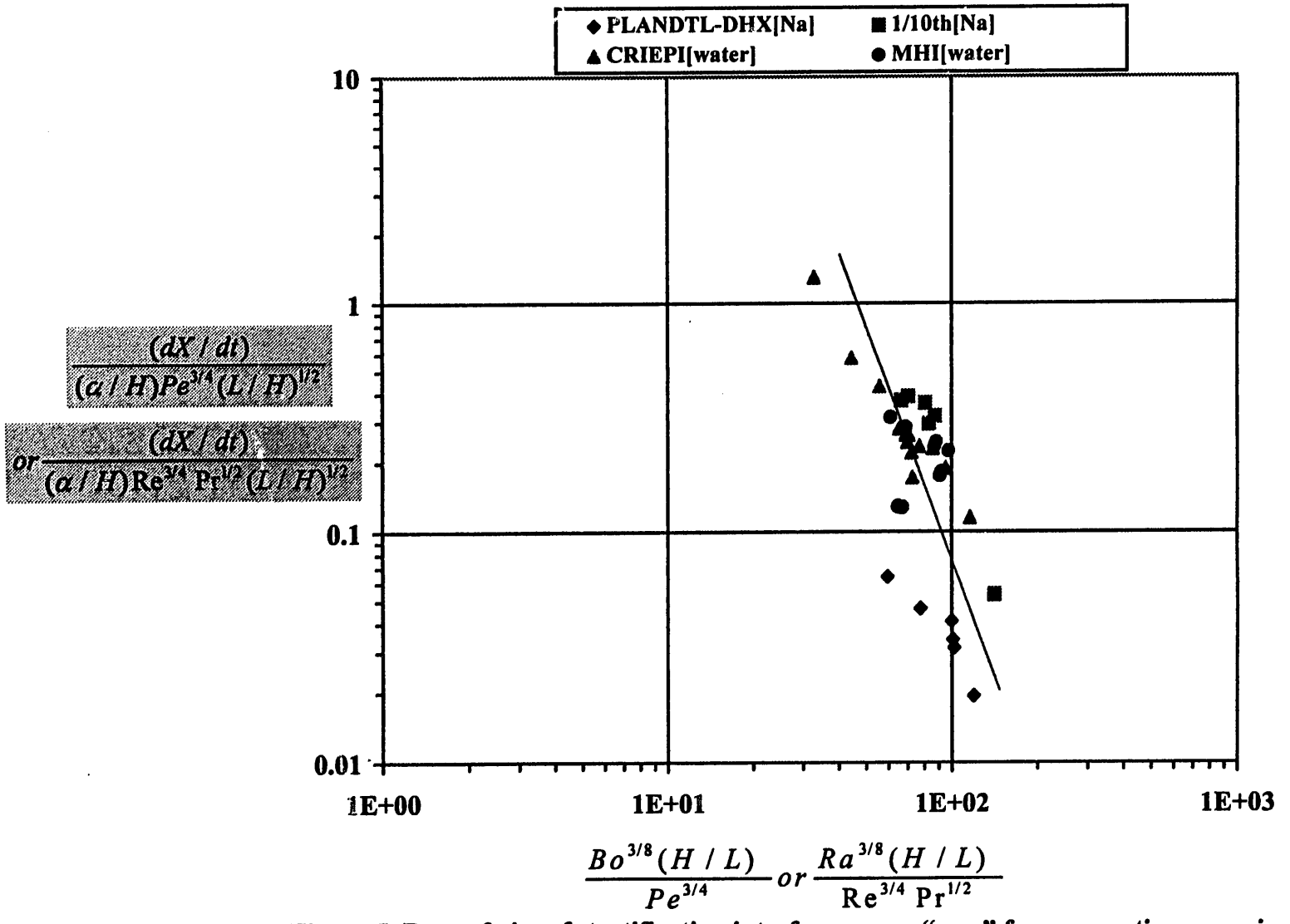

Figure 5. Rate-of-rise of stratification interface versus "new" free convection grouping.

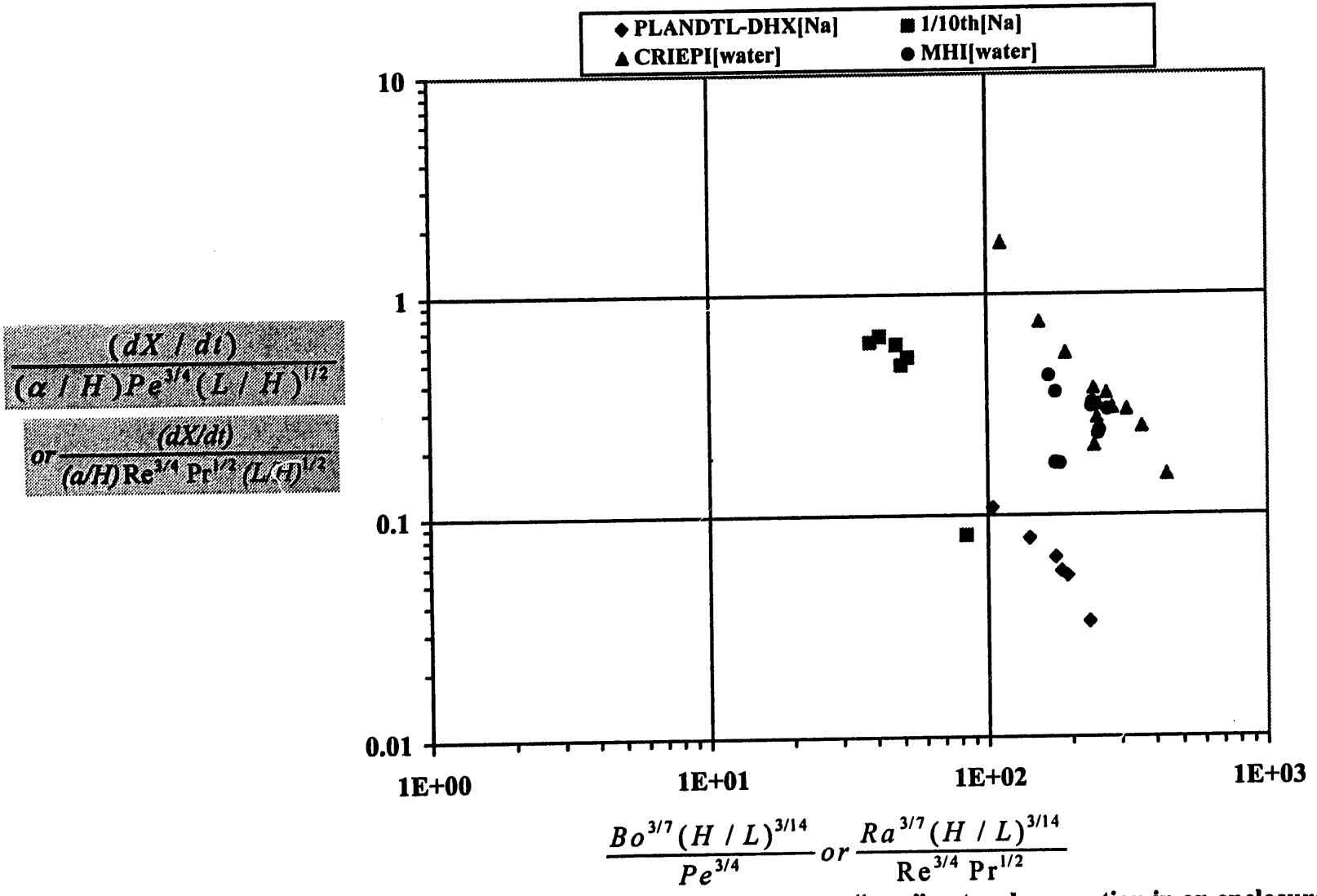

Figure 6. Rate-of-rise of stratification interface versus "new" natural convection in an enclosure grouping.

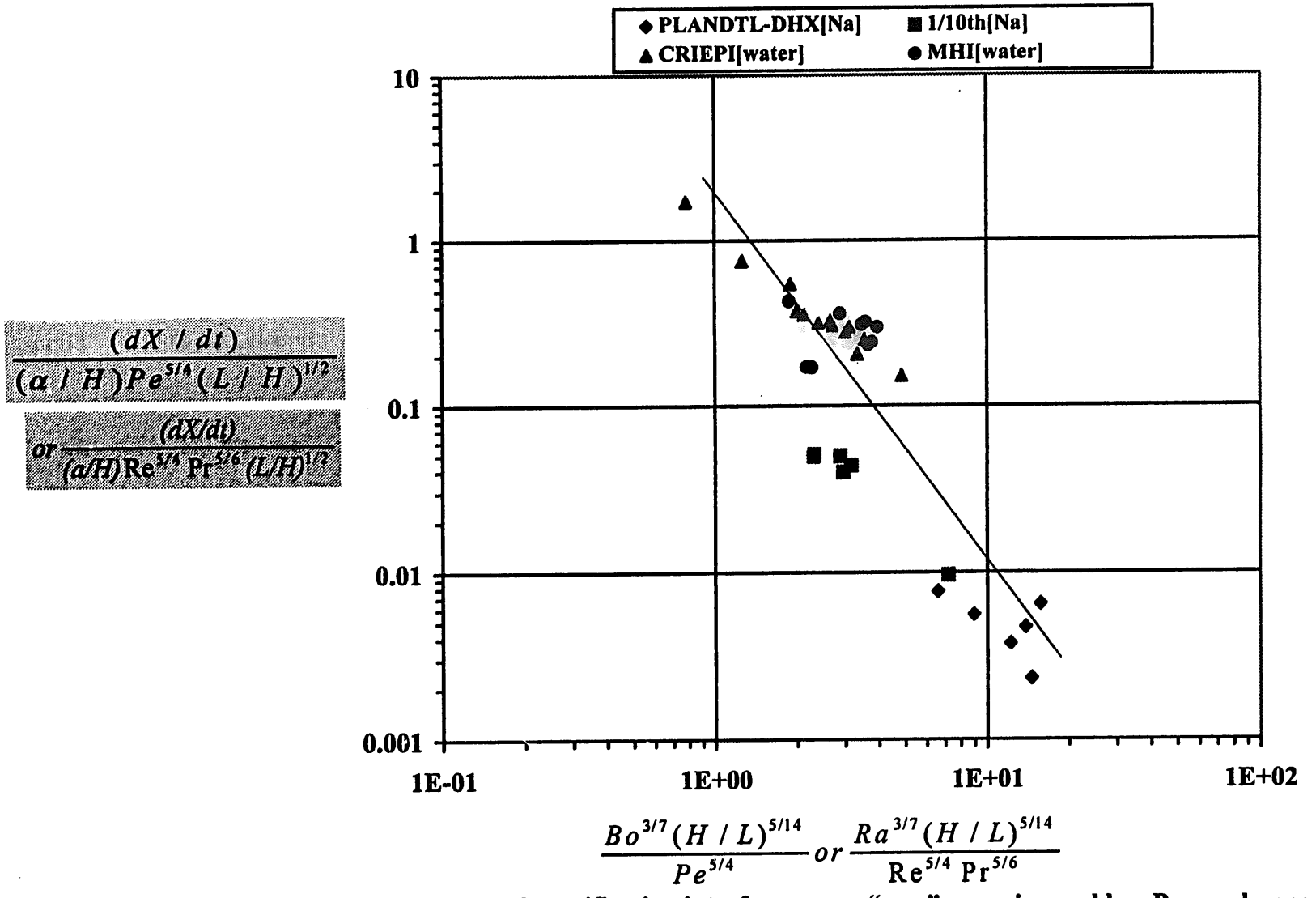

Figure 7. Rate-of-rise of stratification interface versus "new" grouping and low Pr-number correction.

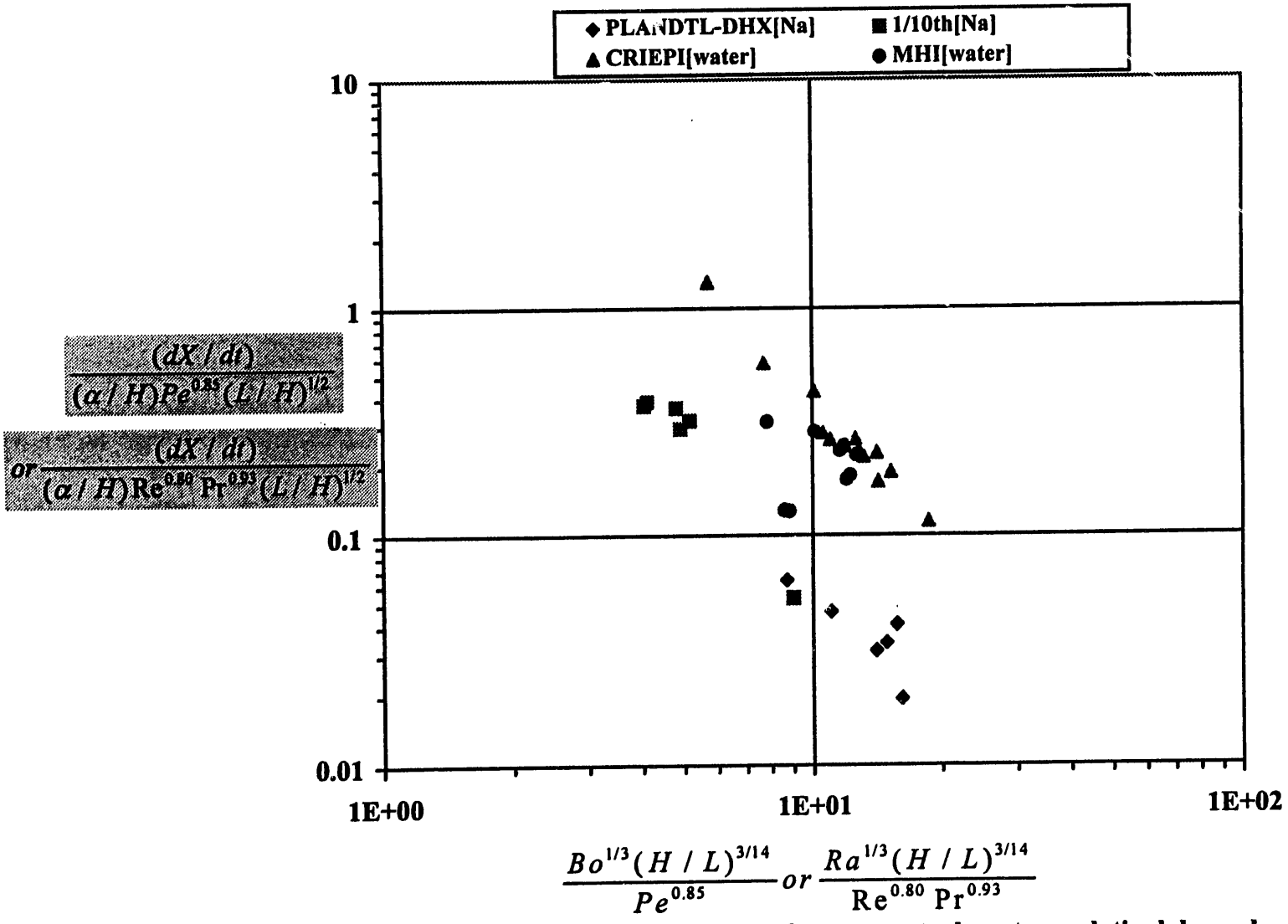

Figure 8. Rate-of-rise of stratification interface versus turbuent correlatinal dependency.

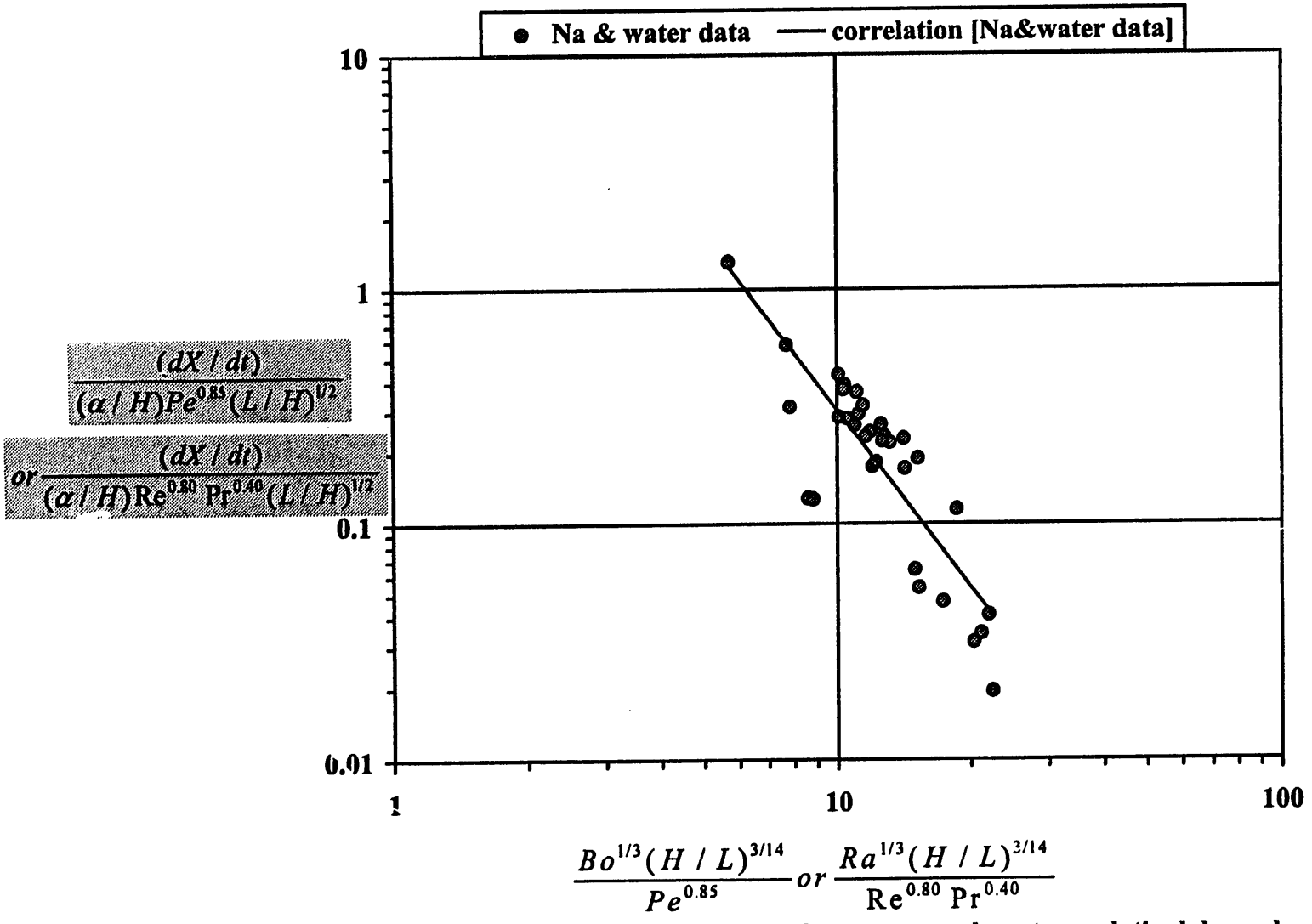

Figure 9. Rate-of-rise of stratification interface versus turbuent correlatinal dependency.